Skyrme-Hartree-Fock treatment of Λ and ΛΛ hypernuclei with *G*-matrix motivated interactions

D. E. Lanskoy
Institute of Nuclear Physics, Moscow State University, 119899 Moscow, Russia

Y. Yamamoto
Physics Section, Tsuru University, Tsuru, Yamanashi 402, Japan

(Received 4 September 1996)

Skyrme-like hyperon-nucleon potentials are derived from *G*-matrix calculations and shown to reproduce well the Λ single-particle spectra of hypernuclei measured at BNL and KEK. Previously known potentials are reexamined systematically. The fit of the spectra can restrict the radii of Λ orbits in hypernuclear ground states, Λ well depth and effective mass in nuclear matter, and polarization of nuclear cores caused by hyperon rather tightly. The implications of the Λ*N* spin-orbit force to the spectra are considered. Hartree-Fock calculations of binding energies of $^{13}_{\Lambda\Lambda}$B with density-dependent *G*-matrix ΛΛ potentials are presented, taking note of the core-rearrangement effects induced by Λ*N* interactions. [S0556-2813(97)01205-3]

PACS number(s): 21.80.+a, 21.10.Dr, 21.60.Jz, 27.20.+n

I. INTRODUCTION

The Skyrme-Hartree-Fock (SHF) approach is known as a powerful and feasible tool for the prediction of gross properties of nonstrange nuclei. Its extension to Λ hypernuclei was performed by Rayet fifteen years ago [1]. However, the reliability of this approach, which is essentially phenomenological, is related directly to the amount of hypernuclear data available. Thus, the reasonable Λ-nucleon Skyrme-like potentials appeared [2–4] subsequently to the first measurement of the Λ hypernuclear energy levels in medium-heavy systems (up to $^{89}_{\Lambda}$Y) done at BNL [5]. The various sets of the potential parameters, which are apparently different from each other, have been proposed and shown to reproduce the experimental spectra equally well. These potentials generally involve a Λ*NN* three-body force or a Λ*N* density-dependent (DD) one, but some of them are purely two body. They predict different values of well depth D_Λ and effective mass m^*_Λ of Λ in infinite nuclear matter.

Recently, the new measurement of Λ hypernuclear spectra by the (π^+,K^+) reaction has been done at KEK [6] for a wide range of nuclear mass numbers (up to $^{208}_{\Lambda}$Pb). The extended amount of data may be used for more tight constraints of the parameters and, more importantly, of the physical quantities describing hyperon properties in the nuclear medium.

The standard form for the two-body Λ*N* Skyrme-like potential is

$$V_{\Lambda N}(\mathbf{r}_\Lambda-\mathbf{r}_N)=t_0(1+x_0P_\sigma)\,\delta(\mathbf{r}_\Lambda-\mathbf{r}_N)+\frac{1}{2}t_1[\mathbf{k}'^2\delta(\mathbf{r}_\Lambda-\mathbf{r}_N)+\delta(\mathbf{r}_\Lambda-\mathbf{r}_N)\mathbf{k}^2]+t_2\mathbf{k}'\,\delta(\mathbf{r}_\Lambda-\mathbf{r}_N)\cdot\mathbf{k}+iW_0\mathbf{k}'\,\delta(\mathbf{r}_\Lambda-\mathbf{r}_N)\cdot(\boldsymbol{\sigma}\times\mathbf{k}) \quad (1)$$

in the conventional notation (see, e.g., [1]). The original SHF approach [1] involves also a Λ*NN* force in the form

$$V_{\Lambda NN}(\mathbf{r}_\Lambda,\mathbf{r}_{N1},\mathbf{r}_{N2})=t_3\delta(\mathbf{r}_\Lambda-\mathbf{r}_{N1})\,\delta(\mathbf{r}_\Lambda-\mathbf{r}_{N2}). \quad (2)$$

The various parameter sets for Eqs. (1) and (2) have been obtained hitherto purely phenomenologically. In this work we propose new parameter sets on the basis of the Λ*N* *G*-matrix calculations with the SU(3)-invariant one-boson-exchange (OBE) potentials, the usefulness of which was established in [7,8]. In our analysis the form of Eq. (2) was found to be not so adequate for representing the density dependence of the Λ*N* *G* matrices. We introduce here a more general form, namely, a Λ*N* force dependent on nuclear density ρ instead of the Λ*NN* force (2):

$$V_{\Lambda N}(\mathbf{r}_\Lambda,\mathbf{r}_N,\rho)=\frac{3}{8}t_3(1+x_3P_\sigma)\,\delta(\mathbf{r}_\Lambda-\mathbf{r}_N)\rho^\gamma\left(\frac{\mathbf{r}_\Lambda+\mathbf{r}_N}{2}\right). \quad (3)$$

The force (3), when $\gamma=1$ and $x_3=0$, leads to Hartree-Fock potentials similar (but not strictly identical [9]) to those of the force (2). In this work we take $\gamma=1/3$, which is found to be adequate to parametrize the *G* matrix result. Note that in the spherical approach used commonly, the spin dependence in velocity-independent pieces (x_0 and x_3 terms) leads to a trivial renormalization of the related amplitudes t_0 and t_3 only.

In Sec. II the *G*-matrix calculation is briefly sketched and the fitting procedure for the Skyrme parameters for Eqs. (1) and (3) is described. Systematic calculations of hypernuclear spectra with new parameter sets as well as previously known ones are discussed in Sec. III. Comparison with the BNL and KEK data shows that our *G*-matrix motivated potentials reproduce the spectra better than the majority of the former sets, though almost no phenomenological fitting is used. Since different parameters lead to similar spectra as usual, we try to find constraints on the physical properties of hypernuclei (D_Λ, m^*_Λ, hypernuclear core polarization, hyperon orbit radii) rather than to search for unique values of the parameters. We also incorporate nonzero spin-orbit (SO) force amplitude W_0 and discuss related implications in view of possible indications of the experimental SO splitting of Λ single-particle levels [10].

In Sec. IV, our SHF scheme is applied to ΛΛ hypernuclei, specifically, to ${}^{13}_{\Lambda\Lambda}$B. As ΛΛ potentials, DD finite-range ones are employed, which simulate the relevant ΛΛ G-matrix interactions. The implicit relation is discussed between the ΛΛ bond energies and the properties of ΛN interactions, especially the *polarizing property*.

Finally, Sec. V includes our conclusions and some outlooks.

II. SKYRME-TYPE PARAMETRIZATION BASED ON THE *G*-MATRIX CALCULATION

First, the G-matrix interactions for a ΛN pair in nuclear matter are derived from the SU(3)-invariant OBE potentials, where the coupling to a ΣN channel is renormalized into the ΛN G matrix. The density dependence (DD) of the resultant G matrix originates from not only the repulsive-core singularity and the tensor force, but also the ΛN-ΣN coupling. The channel-coupled Bethe-Goldstone equation is written as

$$G_{\Lambda N,\Lambda N}=v_{\Lambda N,\Lambda N}+\sum_{Y} v_{\Lambda N,YN}\frac{Q_N}{\omega-T_Y-T_N-\Delta_{Y\Lambda}}G_{YN,\Lambda N}, \tag{4}$$

where Y denotes Λ or Σ and $\Delta_{Y\Lambda}=m_Y-m_\Lambda$. Here the starting energy is given by $\omega=\epsilon_\Lambda+\epsilon_N$, and the Pauli operator Q_N acts on intermediate nucleon states. Adopting here the QTQ prescription for simplicity, we take only kinetic energies T_Y and T_N for intermediate Y and N spectra. An YN relative state is specified by (T,L,S,J) with isospin T and $\mathbf{J}=\mathbf{L}+\mathbf{S}$, which is implicit in the above equation. The potential energy of Λ in nuclear matter is obtained self-consistently in terms of the G matrix as

$$U_\Lambda(k_\Lambda;k_F)=\sum_{\mathbf{k_N}}\langle\mathbf{k}_\Lambda\mathbf{k}_N|G_{\Lambda N,\Lambda N}[\omega=\epsilon_\Lambda(k_\Lambda)+\epsilon_N(k_N)]|\mathbf{k}_\Lambda\mathbf{k}_N\rangle, \tag{5}$$

where k_Λ is the Λ momentum. The Λ single particle energy is given by $\epsilon_\Lambda(k_\Lambda)=\hbar^2k_\Lambda^2/2m_\Lambda+U_\Lambda(k_\Lambda)$. Then, $G_{\Lambda N,\Lambda N}$ and U_Λ are calculated self-consistently for each value of nuclear density ρ (Fermi momentum k_F).

In [7,8], the G-matrix calculations were performed systematically using the various OBE potentials. In order to reproduce the observed data of Λ hypernuclei with the use of the G-matrix interaction, it was indispensable for $U_\Lambda(k_\Lambda=0)$ to be about -30 MeV at normal density ($k_F=1.35$ fm^{-1}). In this work we adopt the Jülich models $\widetilde{A}$ (JA) and $\widetilde{B}$ (JB) [11], and the Nijmegen model F (NF) [12] and the soft-core one (NS) [13], the characters of which are fairly different from each other. JA, JB, and NF lead to $U_\Lambda(k_\Lambda=0)\sim-30$ MeV at $k_F=1.35$ fm^{-1} under the QTQ prescription. On the other hand, the corresponding value for NS is only -23 MeV because of the too small contribution in the ${}^3S_1$ state. It was pointed out that the value of ~-30 MeV is obtained by taking the continuous intermediate spectrum instead of the QTQ one [7,8,14]. However, possibly the latter energy becomes close to the former one by treating the intermediate spectrum self-consistently up to very high momenta [15]. Here we adopt another way of improving the NS potential so that $U_\Lambda(k_\Lambda=0)=-30$ MeV is obtained under the QTQ. In the SU(3) representation, the strong $\{8_a\}$ potential of NS works repulsively (attractively) on $v_{\Lambda N,\Lambda N}$ ($v_{\Lambda N,\Sigma N}$) in the ${}^3S_1$ state, which results in the small contribution to U_Λ in this state. Now we add an attractive correction $v_0\exp[-(r/r_0)^2]$ with $v_0=-240$ MeV and $r_0=0.5$ fm, artificially to the $\{8_a\}$ part of NS. The corrected version is denoted by NS′ in this paper.

TABLE I. Even- and odd-state contributions to $U_\Lambda(k_\Lambda=0)$, $U_\Lambda^{\rm even}$ and $U_\Lambda^{\rm odd}$ as functions of k_F for JA, JB, NF, and NS′ under the QTQ approximation. The values in parentheses are the ratio of the singlet-state contribution in $U_\Lambda^{\rm even}$.

	k_F (fm^{-1})	1.35	1.2	1.0	0.8
JA	$U_\Lambda^{\rm even}$	−30.8	−25.5	−17.6	−10.6
		(0.117)	(0.164)	(0.188)	(0.209)
	$U_\Lambda^{\rm odd}$	1.8	0.78	0.17	0.00
JB	$U_\Lambda^{\rm even}$	−34.9	−28.3	−19.2	−11.5
		(0.014)	(0.063)	(0.083)	(0.096)
	$U_\Lambda^{\rm odd}$	3.6	1.8	0.61	0.16
NF	$U_\Lambda^{\rm even}$	−30.7	−27.4	−20.5	−13.1
		(0.325)	(0.304)	(0.287)	(0.275)
	$U_\Lambda^{\rm odd}$	−0.96	−0.89	−0.57	−0.26
NS′	$U_\Lambda^{\rm even}$	−30.6	−25.6	−18.2	−11.3
		(0.482)	(0.440)	(0.397)	(0.364)
	$U_\Lambda^{\rm odd}$	0.56	0.04	−0.14	−0.10

In Table I the potential energies $U_\Lambda(k_\Lambda=0)$ and the partial wave contributions at some values of k_F are shown in the cases using the above OBE models, where the essential ingredients of the present analysis are included. The ''experimental'' value of about -30 MeV at $k_F=1.35$ fm^{-1} is now reproduced fairly well in these cases within QTQ. However, the ratios of the ${}^1S_0$ and ${}^3S_1$ contributions, relating to the spin-spin interaction parts, are quite different among them. The experimental data, for instance the 0^+ and 1^+ splitting of ${}^4_\Lambda$He (${}^4_\Lambda$H), support the NS′ result [8]. The weak odd-state contributions, seen in Table I, were pointed out to be important for reproducing the mass dependence of Λ binding energies [8]. This is the reason why we did not adopt the Nijmegen model D in the present analysis. Now the contributions to U_Λ in the singlet-even (${}^1S_0$) and triplet-even (${}^3S_1$) states are denoted by $U_\Lambda^{\rm se}$ and $U_\Lambda^{\rm te}$, respectively. Then, the even-state contribution is given by $U_\Lambda^{\rm even}=U_\Lambda^{\rm se}+U_\Lambda^{\rm te}$. The odd-state one $U_\Lambda^{\rm odd}$ is defined similarly.

The Skyrme potential parameters (t_0, x_0, t_1, t_3, x_3, and γ) in Eqs. (1) and (3) are determined so as to reproduce $U_\Lambda^{\rm se}(k_F)$, $U_\Lambda^{\rm te}(k_F)$, and $U_\Lambda^{\rm even}(k_F)$. Additionally we use one experimental value $B_\Lambda({}^{13}_\Lambda{\rm C})=11.69$ MeV (Λ binding energy in the ground state) for fine tuning the parameters. Hereafter we take $\gamma=1/3$ in all cases because the more precise choice of γ leads to no meaningful difference. Our fitting procedure in the simple case of $x_0=x_3=W_0=0$ is as follows. For a trial value of t_1 two parameters (t_0 and t_3) are determined so as to reproduce $U_\Lambda^{\rm even}(k_F)$, and then the SHF calculation for

TABLE II. Skyrme potential parameters derived from the G-matrix calculations, where sets I, II, III, and IV are from JA, JB, NF, and NS′, respectively. Set V is obtained from NS′ with taking account of the LS part. γ is taken as 1/3 in all cases.

No.	t_0 (MeV fm^3)	x_0	t_1 (MeV fm^5)	t_2 (MeV fm^5)	t_3 (MeV fm$^{3+3\gamma}$)	x_3	W_0 (MeV fm^5)
I	−476.0	−0.0452	42.0	23.0	1514.1	−0.280	0.0
II	−422.3	0.2678	98.0	70.0	1219.3	−0.0836	0.0
III	−622.8	−0.0172	116.0	−30.0	1880.3	0.0679	0.0
IV	−542.5	−0.1534	56.0	8.0	1387.9	0.1074	0.0
V	−542.2	−0.1536	58.0	8.0	1383.3	0.1077	62.0

$^{13}_{\Lambda}$C is performed with this set. This procedure is repeated until finding the set to provide $B_\Lambda=11.69$ MeV. In order to fix the values of x_0 and x_3, we perform the fitting procedures separately for $U_\Lambda^{\rm se}(k_F)$ and $U_\Lambda^{\rm te}(k_F)$. On the other hand, the value of t_2 is determined from $U_\Lambda^{\rm odd}(k_F)$. The strength W_0 of the SO part can be obtained also from the G-matrix result by using the Scheerbaum approximation [16]

$$W_0=-2\pi\frac{1}{q}\int_0^\infty r^3 G_{LS}^{\rm to}(r) j_1(\overline{qr})\,{\rm d}r, \tag{6}$$

where $G_{LS}^{\rm to}(r)$ is the SO component of the spatially represented G matrix in the triplet-odd state. We take here $\overline{q}=0.7$ fm^{-1}, but the result is quite insensitive to $\overline{q}$. For the obtained value of W_0, the other parameters are determined by the above procedure. Here the parameter search is performed, instead of using the experimental value of $B_\Lambda(^{13}_{\Lambda}{\rm C})$, so that the value of $B_\Lambda(^{17}_{\Lambda}{\rm O})$ calculated with the SO part is equalized to the one obtained with the corresponding set without the SO part.

In Table II we give the determined parameters. Here sets I, II, III, and IV are obtained from JA, JB, NF, and NS′, respectively, without taking the SO part into account. Set V includes the SO part in the NS′ case. The SO parts in the other cases, not involved here, are fairly smaller than that in the NS′ case. The antisymmetric part [proportional to $\mathbf{L}\cdot(\boldsymbol{\sigma}_\Lambda-\boldsymbol{\sigma}_N)$], not considered here, has to reduce the value of W_0 effectively. It is worthwhile to say that the LS (ALS) part in NS is the strongest (weakest) among those in the above models, which is adequate to demonstrate the role of the SO interaction in our approach. The quantitative treatment for the Λ level SO splitting in hypernuclei is beyond the present work.

In the following section we use also the other sets, III′ and III″, obtained from NF, though their parameters are not given in Table II, in order to demonstrate the relation of the $U_\Lambda^{\rm even}(k_F)$ and $U_\Lambda^{\rm odd}(k_F)$ to the resultant hypernuclear spectra: The set III′ was obtained by combining $U_\Lambda^{\rm even}$ of NF with $U_\Lambda^{\rm odd}$ of JA, and the set III″ was done by multiplying $U_\Lambda^{\rm even}$ by 0.91 with no change of $U_\Lambda^{\rm odd}$. In both cases the total potential energies at $k_F=1.35$ fm^{-1} become almost the same as that for JA.

III. Λ HYPERNUCLEAR SPECTRA

In this section, we consider the hypernuclear properties, mainly energies of Λ single-particle states, in a wide range of mass number A in connection with the features of ΛN potentials. The adopted approach is the same as in [1]. Then, the G-matrix-based potentials from Table II, as well as the previously known parameter sets, are tested by comparing the resultant hypernuclear spectra with the experimental data.

Some earlier parameter sets are listed in Table III. All of them are known to reproduce the spectra measured at BNL satisfactorily. It is notable from Tables II and III that wide ranges of the parameters are allowed.

Before the comparison with the experimental data, the following point should be emphasized. The KEK data used include the published [6] Λ binding energies B_Λ for the $1s$ and $1p$ states as well as the unpublished ones [17] for the

TABLE III. Skyrme potential parameters. All the potentials are in the three-body form (2) except set 4 which is in DD form (3) with $\gamma=1/3$ and $x_3=0$. In Ref. [3], only t_1+t_2 value was presented, and a gradient term linear in $(3t_1-t_2)$ was ignored. It is equivalent to the t_1 and t_2 values as in this table. In this case, t_3 is in MeV fm^4.

No.	t_0 (MeV fm^3)	x_0	t_1 (MeV fm^5)	t_2 (MeV fm^5)	t_3 (MeV fm^6)	Ref.
1	−349.0	−0.108	67.61	37.39	2000	[2]
2	−391.8	−0.085	56.95	48.05	3000	[2]
3	−265.7	−0.216	92.17	12.83	0	[2]
4	−659.0	0	32.5	97.5	2200	[3]
5	−315.3	−0.109	23.14	−23.14	2000	[2]
6	−372.2	−0.107	100.4	79.60	2000	[2]
SKSH1	−176.5	0	−35.8	44.1	0	[4]

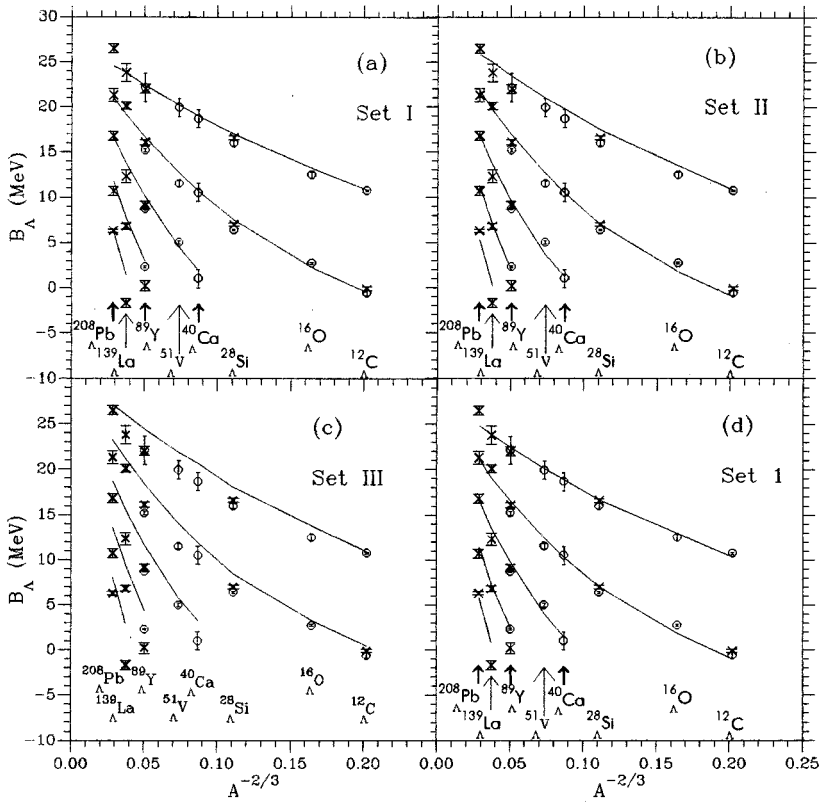

FIG. 1. Calculated Λ binding energies in the $1s$, $1p$, $1d$, $1f$, and $1g$ states (from top to bottom) as functions of $A^{-2/3}$, where A is the mass number of core nucleus, in comparison with KEK [6,17] (×) and BNL [5] (●) data. The ΛN potentials are I (a), II (b), III (c), and 1 (d) from Tables II and III.

$1d$, $1f$, and $1g$ states. The binding energies were evaluated [6,17] by fitting of experimental spectra with the simplest superposition of Gaussians. It means that the main series of the states related to a single neutron hole (with the highest angular momentum) was taken into account for each hypernucleus, neglecting contributions of deeper holes. This prescription avoids additional assumptions about non-major series, which are not justified sufficiently in their fitting procedure. However, it may oversimplify the actual picture. Related uncertainties may be substantial for the high-lying states, and therefore the ''experimental'' values of B_Λ for the $1d$, $1f$, and $1g$ states should be regarded as only rough estimation. Thus, our argument is based primarily on the data [6] for the $1s$ and $1p$ states. Then we incorporate also the data on the high-lying states paying attention to possible uncertainties.

In Figs. 1, 2, and 3, the calculated binding energies B_Λ of Λ hyperons in $1l$ states ($l=s,p,d,f,g$) are shown in comparison with the KEK and BNL data. As the NN potential, the famous Sk3 set [18] is used. One can see that the agreement for the $1s$ and $1p$ states is good for our potentials I [Fig. 1(a)] and II [Fig. 1(b)]. The spectra predicted with the new sets obtained from NS′ (set IV, not shown in the figure) and JA are quite similar to each other (noting that their different spin dependence is beyond the present consideration). The above result indicates that the difference in the DD between NS′ and JA has only a minor effect on the hypernuclear spectra, namely the gross hypernuclear properties are not sensitive to the detail of the adopted OBE potential if $U_\Lambda(k_\Lambda=0)\approx -30$ MeV is reproduced at normal density. There appear characteristically the deviations of the calculated values of $B_\Lambda(1s)$ from the experimental ones: Whereas an overall agreement takes place, the ground state of $^{208}_{\Lambda}$Pb is underbound. Then, the potentials fitted to the $^{13}_{\Lambda}$C ground state such as sets I, II, and IV lead to an overbinding of the $^{16}_{\Lambda}$O ground state. These results are not dependent on the particular choice of the parameters.

Set III from the NF model gives the $1s$ and $1p$ binding energies substantially higher than the experimental ones [Fig. 1(c)] due to high $U_\Lambda(k_\Lambda=0)$, as seen from Table I. This drawback can be cured either by changing the p wave interaction (the set III′) or by reducing the s wave attraction (the set III″). In both of these ways, we obtain a reasonable agreement with the measured values for the $1s$ and $1p$ states.

For the high-lying $1d$, $1f$, and $1g$ states, sets I and IV give similar spectra again. Set II with a higher p wave repulsion predicts higher level spacing, whereas set III leads to, otherwise, small spacing. Evidently, the last feature is retained with set III″, but not with set III′, which indicates that the attractive p-state interaction in set III″ (the same as in set III) is not adequate for higher level spacing. Thus, the high-lying spectra seems to support the almost vanishing (NS′) or slightly repulsive (JA) p-state interaction.

The spectra obtained with set 1 [Fig. 1(d)] are similar to those with sets I and IV, though the level spacing in this case is slightly higher. Each of sets 2, 5, and 6, given in [2] together with set 1, differs from set 1 in a single feature. Namely, set 2 offers a stronger ΛNN force, set 5 is local, and set 6, otherwise, possesses a greater nonlocality. Therefore, set 5 [Fig. 2(a)] leads to smaller level spacing whereas set 6 [Fig. 2(b)] gives a greater one in comparison with sets 1, I, and IV, and likely the sets III and II, respectively. This is exhibited mainly in the high-lying states while the descriptions for the $1s$ and $1p$ binding energies are equally good. Note, that results obtained with the SKSH2 set from [4] (not

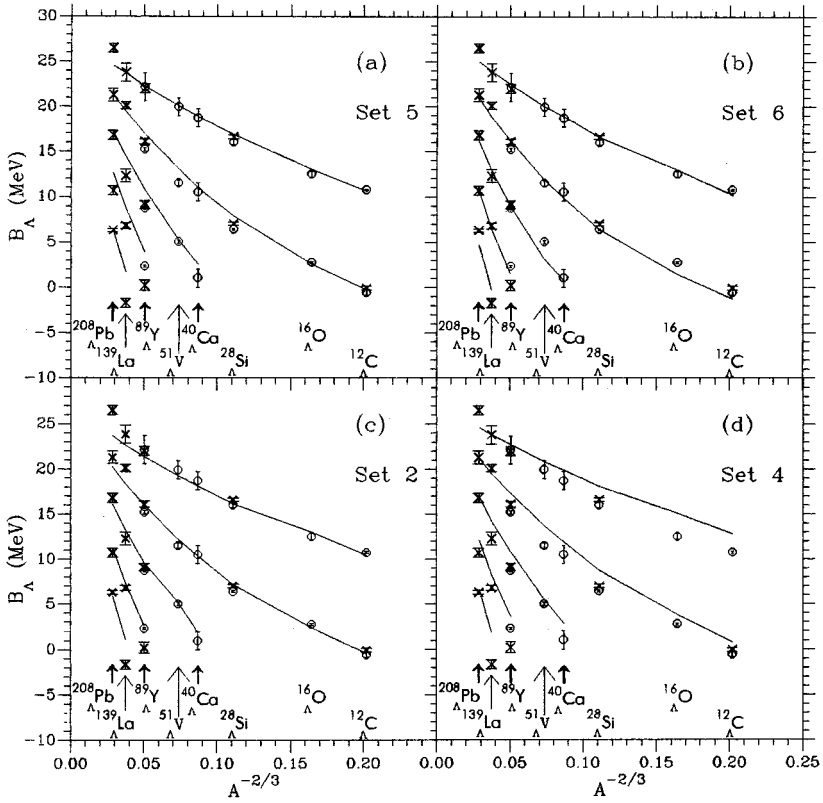

FIG. 2. The same as in Fig. 1 for the ΛN potentials 5 (a), 6 (b), 2 (c), and 4 (d) from Table III.

shown here) are similar to those for set 5. The strong ΛNN force [set 2, Fig. 2(c)] results in an underbinding of ${}^{208}_{\Lambda}$Pb and ${}^{139}_{\Lambda}$La. Though the fit for light and medium hypernuclei is adequate, the overall agreement is poorer.

Set 4 predicts evidently excessive Λ binding in light hypernuclei [Fig. 2(d)]. The same takes place for other nonlocal sets from [3]. It should be noted, however, that another approach, instead of the Hartree-Fock one, has been used in Ref. [3] for the parameter fitting.

Set 3 (not shown) and SKSH1 (Fig. 3) without three-body ΛNN or DD ΛN forces give, first, too large level spacings in light hypernuclei and, secondly, an incorrect A dependence of B_Λ in the ground states. In particular, B_Λ's in the ground states of ${}^{139}_{\Lambda}$La and ${}^{208}_{\Lambda}$Pb are quite close to each other, contrary to the data. Thus, it is shown that these sets are inadequate to reproduce the overall hypernuclear spectra.

We do not use here the quantitative χ^2 criterion for the following reason. The experimental error bars are quite different among the data, and the statistical weights of some particular points are dominantly high. On the other hand, our approach should not be required to ensure the accuracy of 0.1–0.3 MeV achieved in the experiments. So the χ^2 values can possibly misrepresent the picture of the overall fitting.

For illustrative purposes, we show in Table IV the sums of squared deviations $S^2=\Sigma(B_\Lambda^{\rm theor}-B_\Lambda^{\rm exp})^2/(1\ {\rm MeV})^2$ assuming no statistical weights. The KEK data were used for $B_\Lambda^{\rm exp}$ except ${}^{16}_{\Lambda}$O, ${}^{40}_{\Lambda}$Ca, ${}^{51}_{\Lambda}$V, and ${}^{12}_{\Lambda}{\rm C}_{\rm g.s.}$ for which the BNL data were used. Though somewhat arbitrary, the S^2 quantity can be accepted as a reasonable guideline for the overall fitting.

The first line in Table IV corresponds to the $1s$ and $1p$ states only (16 points). It is seen that the potentials I, II, III′, III″, IV as well as 1, 5, and 6 are the most reliable. In the second line, the S^2 values for the full set of data (26 points) are presented. First of all, it is seen from the table as well as from Figs. 1–3 that the fit becomes poorer in all the cases. The greatest contributions to the S^2 are typically from binding energies of ${}^{89}_{\Lambda}{\rm Y}(1f)$ and ${}^{139}_{\Lambda}{\rm La}(1g)$, which are overbound in the calculations. Generally, the calculated level splitting is too small. Therefore, the best S^2 is obtained for sets II and 6. Sets I, 1, and, to a less extent, III′ and IV appear to be satisfactory too, whereas sets III″ and 5 are rejected by these data.

As mentioned above, however, it should be noted that the data for high-lying states may be more or less uncertain. To estimate the effect of these uncertainties, we consider also

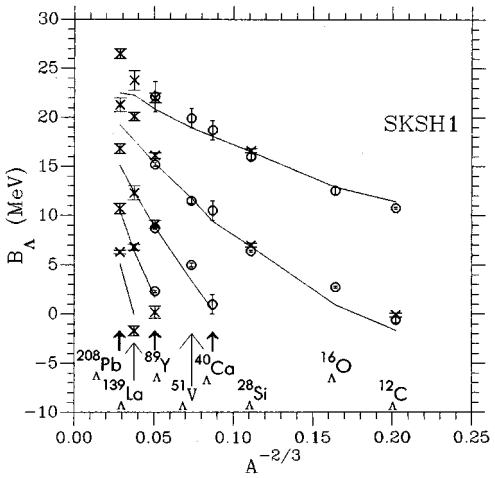

FIG. 3. The same as in Fig. 1 for the ΛN potential SKSH1 from Table III.

TABLE IV. Sums of the squared deviations $S^2=\Sigma(B_\Lambda^{\rm theor}-B_\Lambda^{\rm exp})^2/(1\ {\rm MeV})^2$ for various sets of data (see text).

Potential	I	II	III	III′	III″	IV	1	2	3	4	5	6	SKSH1
	9	12	44	10	15	10	7	16	34	33	9	9	39
S^2	32	24	127	46	88	45	22	32	49	72	62	19	51
	14	20	82	21	46	19	12	22	43	46	27	26	57

the other ''experimental'' values of B_Λ in the $1d$, $1f$, and $1g$ states (not shown in the figures). These values were obtained [19] by the fitting of the same experimental spectra by more complicated curves, involving some theoretical suggestions about deeper hole state contributions. This alternative fit is clearly more model dependent, nevertheless, it may reflect some features of the true picture more completely. In the case of ${}^{89}_{\Lambda}{\rm Y}(1f)$, for instance, the main $g_{9/2}^{-1}$ and minor $f_{5/2}^{-1}$ contributions make the peak double humped where the former (the latter) is of upper (lower) energy, as shown in the DWIA calculation [20]. In [6,17] this possible double-humped peak is fitted as a single peak. Because of such a situation, it is likely that the fitting in [6,17] underestimates the level splitting, especially for the high-lying states.

The S^2 values for the binding energies of the high-lying states from [19] and for the same ones of the $1s$ and $1p$ states as above are shown in the third line of Table IV. First of all, it is seen that the agreement becomes better for all the potentials (except sets 6 and SKSH1) that supports the fitting procedure [19]. So we may suggest that the latter set of B_Λ's is more reliable, though further more consistent analysis is, of course, necessary.

In this case, sets I and 1 are clearly the best, and sets 5 and 6 may be considered as some ''extreme'' cases of the small and great spacing, which are nearly adequate too. The S^2 value of set II is almost the same as that of set IV. It is noted here that the spectra obtained by the latter is similar to the one obtained by set I while set II leads to higher level spacing as mentioned previously. We find also that the large S^2 value of set III (NF) can be improved more remarkably by the readjustment of the p-state part than that of the s-state one. Thus, it is demonstrated that the careful assignment for the observed peaks is indispensable to test the ΛN parameter sets and the underlying G-matrix interactions in detail, especially, to fix the p wave interaction amplitude.

Note that we do not treat set 2 as an adequate one in spite of low S^2 values for the full sets of the data due to the evident qualitative disagreement for heavy hypernuclei. At the same time, this set may be approved for light and medium hypernuclei. It should be emphasized that, particularly in sets 2 and SKSH1, more or less successfully fitting data at $A<89$, fail in the description of ${}^{208}_{\Lambda}$Pb and ${}^{139}_{\Lambda}$La binding energies. It shows that the KEK data in a wide range of A can complement substantially our knowledge of the ΛN interaction.

Summing up, it seems impossible now to extract unambiguously the potential parameters from the B_Λ values obtained by purely phenomenological fitting for the experimental spectra. In spite of this limitation our G-matrix potentials (excepting set III with too attractive p-state interaction) give a reasonable agreement together with sets 1, 5, and 6. Proper assignment of the states observed experimentally, for which some theoretical input will be needed, is quite important for further progress.

The correlation between the values of potential parameters and the quality of the spectra description is not obvious. Even sets I, IV, and 1, giving similar spectra, differ from each other evidently. The experimental data are not enough to fix the potential parameters in detail, which are considered to be determined rather accidentally in the phenomenological fitting. In other words, there are many parameter sets, which are almost equivalent for representing observable quantities. Hereafter, we try to obtain constraints on some physical quantities which can be established independently from the seemingly different parameter values.

In Table V, the Λ binding energy D_Λ and the effective mass m_Λ^* in nuclear matter are shown. Both quantities are calculated at saturation density 0.145 fm^{-3} ($k_F=1.29$ fm^{-1}) as given by the Sk3 potential. [D_Λ is essentially the same as $-U_\Lambda(k_F)$ in Sec. II and deviates from those at $k_F=1.35$ fm^{-1} in Table I.] Next, we consider the polarization of the nuclear core induced by the Λ presence [21,22], called here the *polarizing property*. The core polarization is exemplified by the relative contraction of the nuclear core in the ${}^{16}_{\Lambda}$O ground state $\delta R=(R-R_0)/R_0$, where R and R_0 are the rms radii of the core in ${}^{16}_{\Lambda}$O and ^{15}O, respectively. The polarizing property is driven mainly by three-body ΛNN or DD ΛN force and also by the nonlocality of ΛN interaction. For more details, see [23] and references therein. The two rightmost columns in Table V are the rms radii r_Λ of Λ orbits in the ${}^{16}_{\Lambda}$O and ${}^{208}_{\Lambda}$Pb ground states.

It is seen that the presented quantities are in remarkable

TABLE V. Λ hypernuclear properties calculated with various ΛN potentials from Tables II and III with the Sk3 NN potential ($k_F=1.29$ fm^{-1}).

ΛN	D_Λ (MeV)	m_Λ^*/m_Λ	$\delta R({}^{16}_{\Lambda}{\rm O})$ (%)	$r_\Lambda({}^{16}_{\Lambda}{\rm O})$ (fm)	$r_\Lambda({}^{208}_{\Lambda}{\rm Pb})$ (fm)
I	27.93	0.881	−0.6	2.20	4.06
II	29.85	0.747	−0.5	2.27	4.12
III	30.90	0.848	−0.1	2.28	3.99
III′	28.91	0.815	−0.1	2.31	4.15
III″	28.24	0.962	−0.3	2.22	4.01
IV	28.56	0.882	−0.5	2.22	4.04
1	28.32	0.821	−0.3	2.25	4.10
2	26.94	0.821	+0.1	2.31	4.25
3	30.62	0.821	−1.2	2.12	3.86
4	28.01	0.787	−0.2	2.28	4.36
5	27.48	1.000	−0.5	2.14	3.96
6	28.81	0.728	−0.2	2.31	4.19
SKSH1	25.34	0.983	−1.5	1.99	3.96

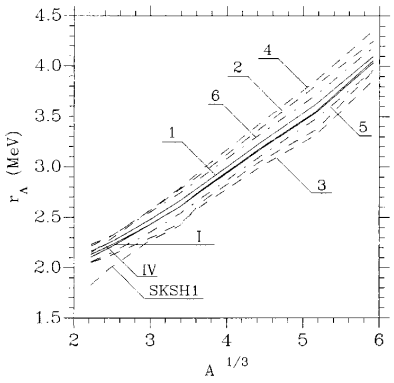

FIG. 4. rms radii of Λ orbits in the ground states of ${}^{A+1}_{\Lambda}$Z hypernuclei as functions of $A^{1/3}$ for the ΛN potentials (labeled in the figure) from Tables II and III.

agreement with the spectra generated by them. The three parameter sets (I, IV, and 1), which reproduce the experimental spectra fairly well and similarly to each other, predict the quantities very close to each other in spite of their seemingly different parameter values. First of all, the radii of the hyperon orbits appear to be restricted rather tightly. It is seen also in Fig. 4, where the A dependence of r_Λ in the ground state is shown. Sets 3, 5, and SKSH1 give systematically smaller r_Λ's, whereas sets 2, 4, and 6 predict, otherwise, larger ones. It should be noted that the former have no three-body ΛNN force (set 3 and SKSH1) or nonlocality (set 5). On the other hand, set 2 (sets 4 and 6) is with a stronger ΛNN force (the larger nonlocality) than the others. One can see that sets I, IV, and 1 envelope just a narrow band for r_Λ's in Fig. 4 (solid lines) and sets 5 and 6 (dot-dashed lines) widen this band to some extent, whereas the potentials found to be inadequate give the radii (dashed lines) mainly beyond these bands. Other G-matrix potentials give the radii, which are more or less close to these bands, though the III and III′ sets lead to a more gradual raising of r_Λ with A. So we obtain some reliable prediction for r_Λ's which can become more accurate when more accurate spectra are available, regardless of a possible ambiguity in potential parameters. A similar picture takes place for the other quantities considered.

We restrict the consideration of the radii to the ground states only, since r_Λ's for near-threshold states are sensitive to slight differences in the binding energies provided by various interactions. Some speculations have been made [24] for the A dependence of r_Λ based on various phenomenological Λ-nucleus potentials, which did not lead, however, to unambiguous predictions. Our r_Λ's in heavy hypernuclei are much larger than those predicted in Ref. [24].

For the well depth D_Λ, we obtain 27.5−29.9 MeV (and a more narrow range 27.9−28.6 MeV, if sets I, IV, and 1 are accepted only). Also the polarizing property of ΛN interaction in these cases appears to induce a slight contraction of the core (about 0.5% in light hypernuclei and about 0.1% in ${}^{208}_{\Lambda}$Pb). Larger contractions connect with smaller r_Λ's and, otherwise, nearly zero polarizations give large Λ orbit radii. And the nonlocality cannot be constrained substantially now because of the uncertainty in the empirical level spacing. The assignment of the high-lying states affects this point most crucially.

TABLE VI. The same as in Table V for the SkM* potential ($k_F = 1.33$ fm^{-1}).

ΛN	D_Λ (MeV)	m^*_Λ/m_Λ	$\delta R({}^{16}_{\Lambda}\mathrm{O})$ (%)	$r_\Lambda({}^{16}_{\Lambda}\mathrm{O})$ (fm)	$r_\Lambda({}^{208}_{\Lambda}\mathrm{Pb})$ (fm)
I	29.27	0.870	−0.8	2.21	3.98
II	31.25	0.722	−0.7	2.28	4.05
III	31.90	0.835	−0.2	2.30	3.93
III′	29.48	0.800	−0.2	2.33	4.10
III″	29.09	0.958	−0.4	2.23	3.95
IV	29.80	0.812	−0.7	2.23	3.96
1	29.16	0.806	−0.5	2.26	4.04
2	26.74	0.806	+0.1	2.32	4.23
3	33.50	0.806	−1.8	2.11	3.76
4	28.24	0.770	−0.3	2.28	4.32
5	28.51	1.000	−0.7	2.15	3.89
6	29.50	0.708	−0.4	2.32	4.14
SKSH1	27.94	0.981	−2.4	1.93	3.84

These constraints for the above physical quantities seem to be rather stable and to reflect true dynamical properties of hypernuclear interactions. However, some uncertainty originates from choice of the NN potential. We repeated the calculations with the SkM* set [25] instead of the Sk3 one. This set is also used widely in nuclear calculations. Its main differences from the Sk3 set are a higher saturation density 0.160 fm^{-3} ($k_F = 1.33$ fm^{-1}) and lower incompressibility. Accordingly, the calculated rms radii of heavy nuclei are somewhat smaller. Empirical radii and binding energies of some nuclei are more compatible with the Sk3 predictions and others agree better with the SkM* calculations.

When the SkM* potential is employed, the quality of overall fitting of hypernuclear spectra with various ΛN interactions does not change significantly from that in the Sk3 case, though some specific binding energies are modified distinctly. However, the D_Λ, m^*_Λ, δR, and r_Λ values are altered substantially (Table VI). For D_Λ, the range 28.5−31.3 MeV is obtained. The effective mass is slightly smaller. The core polarization is enhanced due to the smaller incompressibility. The r_Λ's are nearly the same in light hypernuclei while they are smaller in heavy ones. It should be emphasized that these quantities with the reliable sets remain in narrow ranges which evidently differ from quantities predicted with the other sets.

It is interesting that the pronounced raising of D_Λ (by about 1 MeV) for the SkM* set does not induce a noticeable improvement in reproducing the binding energies of heavy hypernuclei. The B_Λ values in the ${}^{208}_{\Lambda}$Pb ground state increase by only 0.2−0.4 MeV. The reason is that due to smaller Λ orbit radii, the Λ kinetic energy increases together with the well depth, and a partial cancellation occurs. Therefore, the relation between Λ binding energies in heavy hypernuclei and in infinite matter is not as obvious as it seems.

Let us close this section by a brief discussion of set V, which has a nonzero SO ΛN force. In Fig. 5, the calculated binding energies are shown for both lower ($j = l + 1/2$, solid lines) and upper ($j = l - 1/2$, dashed lines) members of the SO doublets. Consistently with [20], the $1f$ splitting of ${}^{89}_{\Lambda}$Y is the largest splitting throughout all the bound Λ states calculated in this work together with the equal splitting of $1g$

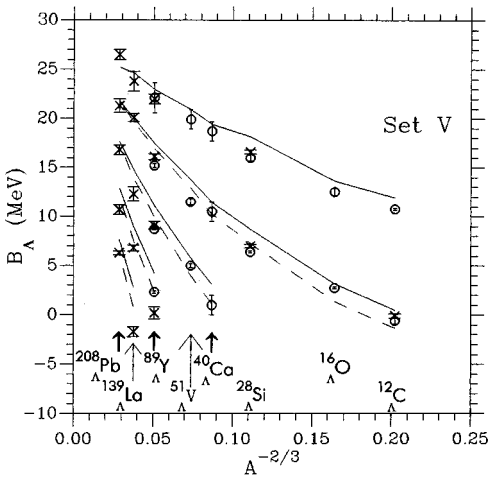

FIG. 5. The same as in Fig. 1 with the ΛN potential V offering nonzero spin-orbit term. Solid (dashed) lines are for the $j=l+1/2$ ($j=l-1/2$) states.

states in $^{139}_{\Lambda}$La. It is seen also that prominent splitting in $1p$ ($1d$) states can be searched for at $A\leqslant 40$ ($40\leqslant A\leqslant 60$).

Of course, it is a problem to compare the calculated spectra directly with the experimental ones, since the data shown in Fig. 5 (the same as in Figs. 1–3) were obtained without supposing any SO splitting. Nevertheless, it is promising that the data points are mostly enclosed by two corresponding lines.

For the splitting in the $^{89}_{\Lambda}$Y $1f$ state, the calculated value 1.9 MeV is obtained which should be compared with the experimental value 2.5 ± 0.2 MeV reported by Nagae [10], though these data are not surely established. We estimated the contribution of the ALS term in the case of NS′ and found the reduction of the above value by a factor 0.8. On the other hand, Motoba *et al.* analyzed recently the level splitting between $[(p_{1/2})_N^{-1}(p_{1/2},p_{3/2})_\Lambda]_{0^+,2^+}$ states of $^{16}_{\Lambda}$O observed in emulsion, and found that the experimental 0^+-2^+ splitting can be reproduced by multiplying by a factor ~ 1.2 on $G_{LS}(r)$ for NS′ without taking the ALS term into account [26]. This indication of the strong LS interaction is quite consistent with the above data of $^{89}_{\Lambda}$Y, because our calculated value 1.9 MeV becomes near to the experimental one by multiplying by a factor of 1.2.

IV. BINDING ENERGY OF $^{13}_{\Lambda\Lambda}$B

Recently, an interest in $S=-2$ hypernuclei has been revived due to the KEK experiments [27,28]. Particularly, a new $\Lambda\Lambda$ hypernucleus, assigned to $^{13}_{\Lambda\Lambda}$B, has been observed [27,29,30].

The $\Lambda\Lambda$ bond energy is defined by $\Delta B_{\Lambda\Lambda}=B_{\Lambda\Lambda}-2B_\Lambda$, where the $B_{\Lambda\Lambda}$ is the separation energy of two Λ's from a $^{A+2}_{\Lambda\Lambda}$Z hypernucleus and the B_Λ is the Λ separation energy from the corresponding $^{A+1}_{\Lambda}$Z hypernucleus. It is known that $\Delta B_{\Lambda\Lambda}$ is sensitive dramatically to the ΛN (or Λ nucleus) interaction and, particularly, to r_Λ [31]. Therefore, an application of the new ΛN interactions is very interesting.

The SHF scheme for $\Lambda\Lambda$ hypernuclei has been presented in [32]. However, the purely phenomenological approach with Skyrme-like $\Lambda\Lambda$ interaction presently encounters considerable uncertainties due to the lack of relevant empirical knowledge. Instead, we use here the $\Lambda\Lambda$ G-matrix interactions [8], which are derived from the $\Lambda\Lambda/\Xi N$ sectors of the Nijmegen OBE models as follows. The $\Lambda\Lambda$-ΞN coupled channel G-matrix equation for a $\Lambda\Lambda$ pair in nuclear matter, similar to Eq. (4), is solved for each nuclear density. The obtained density-dependent $\Lambda\Lambda$ G matrix is represented spatially in a three-range Gaussian form:

$$V_{\Lambda\Lambda}(r)=\sum_{i=1}^{3}(a_i+b_ik_F+c_ik_F^2)\exp(-r^2/\beta_i^2). \qquad (7)$$

The parameters in the $^1S_0$ channel are given in Table VII in the cases of the Nijmegen model D (ND) and NS. Here the hard-core radius (cutoff mass) of ND (NS) is taken in the same way as the one in the corresponding NN channel. It is not so complicated to deal with the finite-range $\Lambda\Lambda$ interactions in our SHF scheme, since exchange $\Lambda\Lambda$ terms do not appear for the ground states. We treat the DD $\Lambda\Lambda$ interaction in the local density approximation. The results appear to be rather insensitive to a specific form of this approximation.

The bond energies $\Delta B_{\Lambda\Lambda}$ calculated with various ΛN and $\Lambda\Lambda$ interactions are listed in Table VIII. It is seen that the ΛN potentials I, IV, and 1 give the bond energies remarkably close to each other. We checked also that the results are insensitive to the choice of NN interaction for these ΛN potentials (but for not all the others). At the same time, the bond energy generally depends on the adopted ΛN interactions via different r_Λ's and different core polarizations. It is seen that the largest deviations from the above reliable values are obtained with the strongly polarizing potentials 3 and SKSH1. However, this dependence is weaker for the DD $\Lambda\Lambda$ interactions than for the density-independent ones.

Considering the results of Table VIII with the use of our reliable ΛN interactions, we see that the NS model clearly underestimates the experimental bond energy 4.9 ± 0.7 [27]. On the other hand, the ND model predicts much more reasonable quantities. Then, it is easy in the case of ND to reproduce the data exactly by taking a smaller value of the hard-core radius. In the case of NS, however, such an adjust-

TABLE VII. Parameters of the $\Lambda\Lambda$ G-matrix potentials in the $^1S_0$ state.

		ND potential			NS potential		
i	β_i (fm)	a_i (MeV)	b_i (MeV fm)	c_i (MeV fm^2)	a_i (MeV)	b_i (MeV fm)	c_i (MeV fm^2)
1	1.5	−10.80	3.029	−1.126	−4.093	0.8137	−0.342
2	0.9	−298.5	156.6	−55.07	−73.45	37.83	−10.19
3	0.5	835.5	−252.7	122.7	75.65	48.54	12.19

TABLE VIII. $\Lambda\Lambda$ bond energies $\Delta B_{\Lambda\Lambda}$ (in MeV) in $^{13}_{\Lambda\Lambda}$B calculated with various combinations of the $\Lambda\Lambda$ and ΛN potentials.

ΛN	ND potential		NS potential
	DD version	density-independent version	
I	3.8	4.3	1.2
II	3.5	4.0	1.2
III	3.4	3.8	1.1
III′	3.4	3.8	1.1
III″	3.7	4.1	1.2
IV	3.7	4.3	1.2
1	3.6	4.0	1.2
2	3.5	3.9	1.2
3	4.4	5.1	1.6
4	3.5	4.0	1.1
5	4.0	4.5	1.2
6	3.4	3.8	1.1
SKSH1	6.1	7.2	2.7

ment is difficult because the resulting $\Lambda\Lambda$ attraction is not so sensitive to the cutoff mass. The present result is similar to the previous three-body (^{11}B$+\Lambda+\Lambda$) calculations [29,8] with the density-independent $\Lambda\Lambda$ interactions which are the same as the DD ones, Eq. (7), fixed at $k_F=1.0$ fm^{-1}. They obtained $\Delta B_{\Lambda\Lambda}=4.7$ MeV with use of the Woods-Saxon-type Λ-core interaction. For comparison, in Table VIII (the second column for the ND model potential) the corresponding results in the present scheme are shown, which are calculated with the same density-independent one. Both results are found to be consistent. It should be pointed out, however, that the value $k_F=1.0$ fm^{-1} is not so adequate as the average Fermi-momentum (k_F) felt by Λ's in the nucleus. We can obtain this quantity in the present scheme as follows. The value of k_F is chosen so that the bond energy in the local density approximation is reproduced in the average density (at k_F) approximation for the specific hypernucleus. Then, we obtained $k_F\approx 1.3$ fm^{-1} regardless of the choice of the potentials, differently from the above value. This means that the Λ's feel a relatively high density in the center of ^{11}B. Of course, this quantity may vary from nucleus to nucleus.

Thus, we argue that the DD of $\Lambda\Lambda$ interaction should not be neglected. The bond energy of two hyperons depends meaningfully on the core central density. Further knowledge on this point can be obtained when other $\Lambda\Lambda$ hypernuclei with different cores (and core central densities) will be observed.

V. SUMMARY AND OUTLOOK

We presented a systematic study of the Λ hypernuclear binding energies in the framework of the Skyrme-Hartree-Fock approach. It was known previously [2,4] that this approach is able to reproduce general properties of single-Λ hypernuclear spectra. The recent KEK experiment [6] enhanced the base for a phenomenological treatment of Λ hypernuclei and allowed us to perform a more accurate analysis.

The hyperon-nucleon interactions suggested here are not purely phenomenological. It appears that G-matrix-motivated parametrization of Skyrme-like ΛN potentials provides a rather good description of the single-Λ spectra when the potential is fitted to two empirical quantities (Λ binding energies in a light hypernucleus and at $A\rightarrow\infty$) only. It may even seem surprising since the free ΛN potentials used are different in their footings and also may be not so accurate due to lack of data on free ΛN interaction. Nevertheless, such a semiphenomenological way appears to be successful. We remark also that it is enough to take account of medium effects via the G-matrix density dependence of the ΛN potential in order to reproduce the experimental spectra, and a genuine ΛNN force is not needed. Only if the condition of $U_\Lambda^{\rm even}\sim -30$ MeV is satisfied, is the quality of fitting to the experimental spectra is insensitive to the detailed density dependence of $U_\Lambda^{\rm even}$. On the other hand, the odd-state contribution is severely restricted due to our analysis: The almost vanishing or the slightly repulsive ones are favorable.

Due to lack of data, seemingly different sets of ΛN Skyrme parameters happen to bring about similar results, and then it is not possible to argue some parameter set as an unique one. This uncertainty makes apparent comparison difficult among various sets. Considering this situation, we try to fix directly some physical quantities. We found some restrictions on Λ properties in nuclear matter together with Λ orbit radii and the core polarization size. Further analysis of the data, including consistent assignment of experimental peaks, can lead to more severe restrictions. There still remains, however, some uncertainty due to ambiguities in core radii and nuclear saturation density and also in nuclear incompressibility. For specific hypernuclei, it is possible to remove this uncertainty using empirical knowledge (though such knowledge is not available for all relevant cores). Spectra of specific hypernuclei may be influenced, of course, also by configuration mixing and some other effects which are beyond our single-particle approach. Since our concern is to study the gross features of the hypernuclear spectra, we did not attempt to specify a nuclear model for each core.

The connection between the binding energies and other hypernuclear features demonstrated here seems to be remarkable. The main obstacle to more definite quantitative conclusions is the uncertainty in the binding energies of the high-lying states. Our calculations provide some preliminary support to the fitting procedure [19] with accounts of deeper hole contributions. On the other hand, it should be emphasized that the proper assignment of the high-lying states is a theoretical rather than experimental task. Strictly speaking, the consistent analysis should start from experimental spectra directly rather than from B_Λ's, and should include calculations of the related cross sections.

Further tests can be searched for in various hypernuclear production rate calculations. Probably, differential cross sections of (K,π), (π,K), and (e,eK) reactions are sensitive to r_Λ's. Also, the nuclear absorption of stopped K^- with strongly peripheral nature should be inspected from this point. Last, pionic weak decay rate is known to be strongly dependent on Λ orbit radii [33].

We examined also the spin-orbit term in the Skyrme ΛN potential. Its amplitude obtained from the Nijmegen-soft-core model gives a fairly smaller value compared to the

recent preliminary experimental indication [10], when both of the *LS* and *ALS* terms are taken into account. For further progress, definite experimental conclusions are needed. In principle, if the states observed now are unresolved spin-orbit doublets, it can disturb the analysis of central interactions too.

We show that the density dependence of the ΛΛ *G*-matrix interaction is not negligible in ΛΛ hypernuclear binding energies. Quantitative treatment of the ΛΛ interaction will be possible in the future when better data are available. On the other hand, the extraction of the ΛΛ potential from relevant hypernuclear data is known to be conditioned crucially by properties of Λ*N* interactions and, particularly, by radii of Λ orbits and polarizing property of a Λ*N* potential (for the most recent discussion see [32,34]). So our study of single-Λ hypernuclei is pertinent also for ΛΛ hypernuclei and ΛΛ interaction problems, and it provides a reliable base for calculations of various ΛΛ hypernuclei.

ACKNOWLEDGMENTS

We would like to express our thanks to Professor O. Hashimoto, Professor T. Nagae, and Dr. T. Hasegawa for providing us their unpublished data and useful comments. We thank Professor T. Motoba for his critical reading of the manuscript. One of the authors (Y.Y.) is supported by a Grant-in-Aid for Scientific Research (C) of the Japan Ministry of Education, Science and Culture (07640418).

[1] M. Rayet, Nucl. Phys. **A367**, 381 (1981).
[2] Y. Yamamoto, H. Bandō, and J. Žofka, Prog. Theor. Phys. **80**, 757 (1988).
[3] D. J. Millener, C. B. Dover, and A. Gal, Phys. Rev. C **38**, 2700 (1988).
[4] F. Fernández, T. López-Arias, and C. Prieto, Z. Phys. A **334**, 349 (1989).
[5] P. H. Pile *et al.*, Phys. Rev. Lett. **66**, 2585 (1991).
[6] T. Hasegawa *et al.*, Phys. Rev. C **53**, 1210 (1996).
[7] Y. Yamamoto and H. Bandō, Prog. Theor. Phys. Suppl. **81**, 42 (1985).
[8] Y. Yamamoto, T. Motoba, H. Himeno, K. Ikeda, and S. Nagata, Prog. Theor. Phys. Suppl. **117**, 361 (1994).
[9] D. E. Lanskoy and T. Yu. Tretyakova, Yad. Fiz. **49**, 1595 (1989) [Sov. J. Nucl. Phys. **49**, 987 (1989)].
[10] T. Nagae, in *Nuclear and Particle Physics with Meson Beams in the 1 GeV/c Region*, Proceedings of the 23rd INS International Symposium, Tokyo, edited by S. Sugimoto and O. Hashimoto (Universal Academy Press, Tokyo, 1995), p. 175.
[11] A. Reuber, K. Holinde, and J. Speth, Nucl. Phys. **A570**, 543 (1994).
[12] M. M. Nagels, T. A. Rijken, and J. J. de Swart, Phys. Rev. D **15**, 2547 (1977); **20**, 1633 (1979).
[13] P. M. M. Maessen, T. A. Rijken, and J. J. de Swart, Phys. Rev. C **40**, 2226 (1989).
[14] H.-J. Schulze, A. Lejeune, J. Cugnon, M. Baldo, and U. Lombardo, Phys. Lett. B **355**, 21 (1995).
[15] S. Nagata (private communication).
[16] R. R. Scheerbaum, Nucl. Phys. **A257**, 77 (1976).
[17] T. Hasegawa, O. Hashimoto, and T. Nagae (private communication).
[18] M. Beiner, H. Flocard, N. V. Giai, and P. Quentin, Nucl. Phys. **A238**, 29 (1975).
[19] T. Hasegawa, Ph.D. thesis, University of Tokyo, 1994.
[20] T. Motoba, Nuovo Cimento A **102**, 345 (1989).
[21] H. Feshbach, in *Proceedings of the Summer Study Meeting on Kaon Physics and Facilities, Brookhaven, 1976*, edited by B. Palevsky, Brookhaven National Laboratory Report No. BNL-50579, 1976, p. 391.
[22] J. Žofka, Czech. J. Phys. B **30**, 95 (1980).
[23] D. E. Lanskoy and T. Yu. Tretyakova, Yad. Fiz. **49**, 401 (1989) [Sov. J. Nucl. Phys. **49**, 248 (1989)].
[24] C. G. Koutroulos, J. Phys. G **17**, 1069 (1991); C. G. Koutroulos and G. J. Papadopoulos, Prog. Theor. Phys. **90**, 1039 (1993).
[25] J. Bartel, P. Quentin, M. Brack, C. Guet, and H. B. Håkansson, Nucl. Phys. **A386**, 79 (1982).
[26] R. H. Dalitz, D. H. Davis, T. Motoba, and D. N. Tovee (in preparation); T. Motoba, Sozyushizon Kenkyu **94**, B53 (1996); T. Motoba (private communication).
[27] S. Aoki *et al.*, Prog. Theor. Phys. **85**, 1287 (1991).
[28] K. Imai, Nucl. Phys. **A547**, 199c (1992).
[29] Y. Yamamoto, H. Takaki, and K. Ikeda, Prog. Theor. Phys. **86**, 867 (1991).
[30] C. B. Dover, D. J. Millener, A. Gal, and D. H. Davis, Phys. Rev. C **44**, 1905 (1991).
[31] A. R. Bodmer, Q. N. Usmani, and J. Carlson, Nucl. Phys. **A422**, 510 (1984); A. R. Bodmer and Q. N. Usmani, *ibid.* **A463**, 221c (1987).
[32] D. E. Lanskoy, in [10], p. 281.
[33] Y. Kurihara, Y. Akaishi, and H. Tanaka, Prog. Theor. Phys. **71**, 561 (1984).
[34] D. E. Lanskoy, Yu. A. Lurie, and A. M. Shirokov, Z. Phys. A **357**, 95 (1997).